



Published in final edited form as:

*Biotechnol Prog.* 2013 September ; 29(5): 1255–1264. doi:10.1002/btpr.1761.

## Hydrolytically Degradable Poly(Ethylene Glycol) Hydrogel Scaffolds as a Cell Delivery Vehicle: Characterization of PC12 Cell Response

Silviya P. Zustiak<sup>\*</sup>, Stephanie Pubill, Andreia Ribeiro, and Jennie B. Leach

Department of Chemical & Biochemical Engineering, UMBC, 1000 Hilltop Circle, Baltimore MD 21250

### Abstract

The central nervous system (CNS) has a low intrinsic potential for regeneration following injury and disease, yet neural stem/progenitor cell (NPC) transplants show promise to provide a dynamic therapeutic in this complex tissue environment. Moreover, biomaterial scaffolds may improve the success of NPC-based therapeutics by promoting cell viability and guiding cell response. We hypothesized that a hydrogel scaffold could provide a temporary neurogenic environment that supports cell survival during encapsulation, and degrades completely in a temporally controlled manner to allow progression of dynamic cellular processes such as neurite extension. We utilized PC12 cells as a model cell line with an inducible neuronal phenotype to define key properties of hydrolytically-degradable poly(ethylene glycol) hydrogel scaffolds that impact cell viability and differentiation following release from the degraded hydrogel. Adhesive peptide ligands (RGDS, IKVAV or YIGSR), were required to maintain cell viability during encapsulation; as compared to YIGSR, the RGDS and IKVAV ligands were associated with a higher percentage of PC12 cells that differentiated to the neuronal phenotype following release from the hydrogel. Moreover, among the hydrogel properties examined (e.g., ligand type, concentration), total polymer density within the hydrogel had the most prominent effect on cell viability, with densities above 15% w/v leading to decreased cell viability likely due to a higher shear modulus. Thus, by identifying key properties of degradable hydrogels that affect cell viability and differentiation following release from the hydrogel, we lay the foundation for application of this system towards future applications of the scaffold as a neural cell delivery vehicle.

### Keywords

Neurotransplantation; stem cells; cell viability; neurite extension; differentiation

### Introduction

Injury and disease in the central nervous system (CNS) can be devastating due to low intrinsic potential for regeneration. One potential strategy for treating these conditions employs neural stem/progenitor cell (NPC) transplants, which have shown promise for ameliorating damage in the CNS but are associated with drawbacks such as low post-implant survival.<sup>1, 2</sup> Biomaterial scaffolds have the potential to provide a defined three-dimensional (3D) microenvironment to guide stem cell response, but unfortunately, the optimal design for such scaffolds is undefined.

Corresponding author: Jennie B. Leach, jleach@umbc.edu, phone: 410-455-8152.

<sup>\*</sup>Current affiliation: Department of Biomedical Engineering, Saint Louis University, 3507 Lindell Blvd, St Louis, MO 63103

Recent studies of NPC transplants have been carried out by injecting a suspension of cells in a buffered solution into the area of nerve injury. This simple approach has provided key insights and new hypotheses about how to improve the success of NPC-based therapeutics. First, the implant environment plays a critical role in influencing NPC fate: NPCs transplanted into “neurogenic” regions of the brain differentiate into region-specific neuronal subtypes, whereas NPCs transplanted into “non-neurogenic” regions generate only glia.<sup>3</sup> While it is likely that cellular, soluble and matrix-based cues all influence the neurogenic potential of these environments, a functional neurogenic environment has yet to be synthesized. Second, lineage-restricted NPCs provide many advantages over undifferentiated stem cells because of their greater survival rates following implantation and their capacity for pre-selection of certain cell subclasses according to disease-specific needs.<sup>4</sup> Thus, the success of NPC therapeutics will be increased by scaffolds that provide cues that are neurogenic and promote differentiation towards a defined subclass population.

Biomaterials scientists have hypothesized that engineered scaffolds are ideally suited to promote nerve repair by filling the cystic cavity, promote guided cell migration and neurite outgrowth and ultimately degrade completely to prevent potentially harmful effects such as compression, scarring, or chronic inflammation.<sup>5, 6</sup> However, biomaterials must be designed to elicit outcomes specific to the particular injury type and location. For example, guided cell migration and neurite outgrowth is of clear benefit to the repair of damaged peripheral nerve and spinal cord, where tissue organization is relatively straightforward and well understood. In the brain, however, the organization of cells and their processes is highly complex and the optimal architecture to promote repair is yet unclear.

Recently, biodegradable polyethylene glycol (PEG)-based hydrogels alone<sup>7</sup> or in conjunction with other polymers<sup>8-10</sup> have been proposed as a promising cell carrier material for neural transplantation. PEG is a suitable polymer for several reasons. First, the mechanical properties (e.g., modulus) of PEG can be controlled to match that of brain tissue (several hundred Pa<sup>11</sup>). As PEG is an inert polymer and has a nanometer mesh size upon cross-linking, it has the potential to decrease the immunogenicity of the implanted tissue<sup>12</sup> thus minimizing the risk of acute neural transplant rejection.<sup>13</sup> Finally, degradable PEG matrices with PEG precursor polymer of low molecular weight, have the ability to degrade over time as the new tissue forms without accumulation of degradation products in the patient.<sup>14</sup>

In this work, we hypothesized that a biomaterial scaffold could provide a temporary neurogenic environment that supports cell survival during encapsulation, while preserving the cells' ability to differentiate to a specific cell subclass, and degrades completely to allow for cell delivery.<sup>13</sup> To test our hypothesis, we applied a hydrolytically-degradable hydrogel scaffold, recently reported by our laboratory,<sup>15, 16</sup> to provide a homogeneous encapsulation environment that forms a hydrogel under physiological conditions and yields a scaffold with tunable physical and biochemical properties. Herein, we describe our initial studies focused on the identification of hydrogel properties that promote PC12 cell viability during encapsulation and differentiation to a neuronal phenotype following hydrogel degradation and release of the cells into the culture environment. PC12 cells were selected as a neuronal cell model because their differentiation may be influenced by soluble cues such as nerve growth factor (NGF)<sup>17</sup> as well as insoluble cues such as extracellular matrix ligands.<sup>18</sup> In this preliminary study, we demonstrate that these hydrogels are suitable for cell encapsulation, thus indicating their potential to serve as cell carriers for neurotransplantation.

## Materials and methods

### Cell maintenance

PC12 cells (ATCC, Manassas, VA) cells were cultured in Dulbecco's Modified Eagle's medium (DMEM; Thermo Scientific, Logan, UT) enriched with 10% fetal bovine serum, 100 µg/ml penicillin-streptomycin, and 5% horse serum at 37°C and 5% CO<sub>2</sub>.<sup>19</sup> Cells were removed from cell culture substrates using 0.05% trypsin/0.02% EDTA (Invitrogen, Carlsbad, CA). Prior to each experiment, cells were primed with 7S NGF (Chemicon) for 48 h.

### Preparation of culture system

To test the ability of the PEG hydrogels to support PC12 cell viability and differentiation, we encapsulated cells within the hydrogels and cultured the resultant scaffolds on top of collagen-coated coverslips. As the hydrogels degraded, cells were released into the surrounding culture environment. Viable cells attached to the underlying adhesive collagen substrate and continued to differentiate accordingly, where the adhesive coverslip mimicked a model neurogenic environment. This section describes the synthesis of the hydrogel and collagen-coated coverslips that comprise the culture system. The subsequent sections describe the cell experiments.

4-arm poly(ethylene glycol)-vinyl sulfone (4-arm PEG-VS) and the cross-linker PEG-diester-dithiol were synthesized following previously described procedures.<sup>16</sup> To prepare the hydrogels, 20 kDa 4-arm PEG-VS 20 was dissolved in triethanolamine (TEA) buffer (0.3 M, pH 8) and cell-adhesive ligand, namely GRCD-*RGDS*-PD, GRCD-*IKVAV*-PD or GRCD-*YIGSR*-PD (CPC Scientific Inc., San Jose, CA), was added at a large stoichiometric deficit of ligand to VS groups on PEG-VS (Fig. 1).<sup>20</sup> The ligands were terminated with the sequence GRCD, which contains a cysteine residue to allow for covalent attachment to PEG-VS.<sup>21</sup> To minimize weighing error, the ligand was aliquoted in advance in 5% acetic acid solution. The acidic solution was used to allow for protonation of the cysteine thiols and thus prevent the formation of disulfide bonds between the ligands. The ligand was left to react with PEG-VS for 15 min and then PC12 cells, suspended in DMEM medium containing 50 ng/ml NGF, were added and the solution mixed thoroughly. Finally, hydrolytically degradable PEG-diester-dithiol cross-linker was dissolved in TEA and added in sufficient quantity to bring the final solution volume to 100 µl and total VS:SH to 1:1. The solution was mixed for 30 sec and 20 µl hydrogels were pipetted on coverslips positioned at the bottom of a 24 well-plate. The hydrogels were incubated at 37°C for 30 min to allow complete gelation. The hydrogels remained attached to the coverslips until complete hydrogel degradation.

The hydrogel was rendered hydrolytically degradable by means of ester containing PEG cross-linker. To manipulate hydrogel properties such as degradation rate, several cross-linkers were explored: PEG-diester-dithiol with varying numbers of methylene groups between the thiol and ester moieties (represented by "m" in Fig. 1) and 3 molecular weights (3.4, 6 and 8 kDa; provided by varying the number of PEG monomer repeat units, which is represented by "n" in Fig. 1). The structure is designated in the cross-linker name: for example, "PEG-SH 2 3.4" corresponds to PEG-diester-dithiol with 2 methylene groups between the thiol and ester moieties and has a molecular weight of 3.4 kDa. We have previously shown that while initial hydrogel properties are similar for all cross-linkers used herein, hydrogel degradation rate was correlated with linker molecular weight (i.e., higher molecular weight cross-linkers caused faster hydrogel degradation) and hydrogels made with cross-linkers with 1 methylene group between the thiol and ester moieties degraded faster than cross-linkers with 2 methylene groups.<sup>16</sup>

To prepare collagen-coated coverslips, type I collagen (from rat tail, 3.75 mg/ml, BD Biosciences, Bedford, MA) was diluted in 0.02 N acetic acid to a final concentration of 50  $\mu\text{g/ml}$ . The solution was then spread on a 12-mm coverslip until the surface was completely covered ( $\sim 7 \mu\text{g/cm}^2$ ). After incubating the coverslips at room temperature for 1 h, the unbound collagen solution was aspirated. The coverslips were rinsed twice with phosphate-buffered saline (PBS) to remove remaining acid and used immediately or stored at 2–8°C for up to 1 wk.

### Cell viability in the hydrogel scaffolds

A LIVE/DEAD cell assay (Invitrogen) was used according to the manufacturer's instructions to assess the viability of cells encapsulated within the hydrogel scaffolds. First, PC12 cells were incubated with a fluorescent green membrane stain (DiOC<sub>18</sub>) for 24 h and then mixed into the hydrogel solution prior to gelation. The final cell concentration was 2,500 cells/ $\mu\text{l}$  hydrogel. Controls included PC12 cells (35,000 cells/ $\text{cm}^2$ ) cultured on standard tissue culture polystyrene or collagen-coated coverslips. All cells were cultured for an additional 24 h at which point a fluorescent red nucleolus stain (propidium iodide, PI; 7.5  $\mu\text{M}$ ) was added to label the dead cells. After incubation for 1 h, images of the cultures were captured under fluorescence microscopy (Olympus IX81, Center Valley, PA) and image analysis was performed using NIH Image-J freeware. Percent cell viability was calculated as the number of live cells divided by the total number of cells  $\times 100\%$ . The samples were not washed before or after adding propidium iodide; thus the analysis considers all cells that were present at the end of the culture period. 50 ng/ml of 7S NGF was added to all samples unless otherwise noted.

### PC12 cell delivery from the hydrogel scaffolds

To test cell delivery from the developed hydrogels, all hydrogels were synthesized with PEG-SH 1 3.4 cross-linkers, 5% w/v total polymer, 100  $\mu\text{M}$  ligand and 50 ng/ml NGF. The hydrogels were observed periodically to determine the time of complete hydrogel degradation ( $\sim 2\text{--}3$  d) and then the cultures were incubated for an additional 48 h, and subsequently fixed for 20 min in 4% formaldehyde. The formaldehyde solution was then removed and replaced with 1 ml of PBS. Cells were imaged immediately or stored in the dark at 2–8°C for up to 2 wks.

### Immunocytochemistry

The samples were washed with PBS, blocked in 10% lamb serum in PBS for 30 min and then incubated in a fluorescently-conjugated primary antibody against tubulin ( $\alpha$ -tubulin-Alexa 488, Invitrogen) and also in phalloidin-Texas Red X (Invitrogen) to label actin; 4',6-diamidino-2-phenylindole (DAPI, 300 nM, Sigma Aldrich) was used to visualize cell nuclei. All procedures were carried out at room temperature.

### Neurite length analysis

The PC12 cells were embedded in the hydrogel scaffolds containing adhesive ligands and cultured on top of collagen-coated coverslips until complete hydrogel degradation ( $\sim 2\text{--}3$  d) and then an additional 48 h. The cells were fixed, stained for tubulin, actin and cell nuclei and then imaged. The lengths of the individual neurites for each cell were measured according to previously described methods.<sup>22</sup> Briefly, neurites longer than 10  $\mu\text{m}$  were traced and the entire length including branches was measured using ImageJ. For each experiment, 4 hydrogels were prepared with each ligand type. For each ligand type, 10 – 20 images of the coverslip surface were randomly acquired. Experiments were repeated on at least 2 separate days.

## Statistical analysis

To assess the statistical significance of differences between the results, 1-way ANOVA was applied for parametric statistics and Kruskal-Wallis was applied for nonparametric statistics, followed by post-hoc analysis. A significance level of  $p < 0.05$  was used.

## Results and Discussion

The goal of this work was to optimize a hydrogel scaffold for the delivery of neural-like cells *in-vitro* as a stepping stone towards a broader future goal of delivering stem cells *in-vivo* for nerve repair or treatment of neurodegenerative diseases. We aimed to define a hydrogel scaffold that promotes high cell viability during encapsulation and also supports differentiation to the neuronal phenotype following release from the hydrogel. Recently, it has been recognized that biomaterials may improve the success of neural stem cell therapies as they have the potential to support high cell viability, attachment, proliferation and ultimately, lineage-specific differentiation.<sup>23–25</sup> Most importantly, material properties such as cytocompatibility to stem cells,<sup>26</sup> modulus,<sup>27, 28</sup> and dimensionality,<sup>29</sup> as well as cell density<sup>30</sup> and cell-matrix interactions<sup>31</sup> have been found to impact profoundly neuronal proliferation and differentiation. Thus, we investigated a number of hydrogel synthesis and culture parameters (e.g., ligand type and concentration, cross-linker type, polymer density, cell density, culture time) in order to identify factors which significantly affect cell viability or cell fate.

Before discussing specific structure-function relationships in detail, we note two general findings: First, all tested hydrogels degraded 3–7 times slower when they contained encapsulated cells versus cell-free hydrogels (by observation only). Similar observations had been made when encapsulating chondrocytes in a hydrolytically degradable PEG-poly(lactic acid) (PLA) hydrogels.<sup>32</sup> This difference was attributed to the considerably lower water content in the scaffolds containing cells versus the scaffolds without cells, which in turn altered the kinetics of the hydrolysis. Second, the PC12 cells in all hydrogel types maintained a spherical morphology and did not extend neurites while encapsulated (data not shown). This finding was not altogether surprising because of the comparative sizes of the hydrogel mesh size – nanometers (initially as well as near complete hydrogel degradation;<sup>16</sup> see also Table 1), and the diameter of the PC12 cells – micrometers, possibly rendering the hydrogel mesh a physical barrier against process extensions. Similarly, other researchers have shown that cells maintain a spherical morphology in 3D cultures as opposed to a flattened or spread morphology in 2D cultures.<sup>33</sup> In PEG hydrogels specifically, fibroblast cells had been shown to elongate only in the presence of enzymatically degradable cross-linkers but not in the non-degradable materials.<sup>34</sup> In contrast to our work, Mahoney et. al. had demonstrated that neural cells are capable of extending neurites after 2 weeks of culture in hydrolytically degradable PEG hydrogels.<sup>7</sup> However, the authors acknowledged that the mesh size at 2 weeks should still be in the order of nanometers (~15 nm) and thus, impermissible to neurites, and attribute the paradox to the heterogeneity in cross-linking density when gelation occurred in the presence of cells. They suggested that a possible contributor to these heterogeneities could be incomplete cross-linking due to cells terminating radicals formed during UV exposure (used to initiate gelation) via the production of antioxidants.<sup>35</sup> Therefore, the lack of cell spreading in our system could be an indicator of a more homogeneous hydrogel structure in the presence of cells, as a result of the physiologically relevant cross-linking conditions that do not require UV irradiation.

Nonetheless, once the PC12 cells were released from the PEG hydrogels, the cells attached to the collagen-coated coverslips and extended neurites comparable to the controls (polystyrene and collagen-coated glass alone). Effects of system parameters on the viability



of encapsulated cells and differentiation to the neuronal phenotype following release are described in the following sections.

### Effects of ligand type and density on PC12 cell viability

The peptide ligands RGDS, IKVAV, and YIGSR were selected because they represent the cell-adhesive domains of fibronectin, collagen and laminin.<sup>15</sup> While these ligands have been shown to support cell adhesion and neurite extension in similar systems, their effect on neuronal cell viability has been examined less often.<sup>36, 37</sup> To determine whether the presence of adhesive ligand was required to maintain cell viability during encapsulation, we compared the viability of PC12 cells in hydrogels with 100  $\mu\text{M}$  ligand versus hydrogels with no ligand (Fig. 2a). Cells encapsulated in hydrogels with adhesive ligand were 90–95% viable, but in hydrogels lacking adhesive ligand, viability dropped to ~ 2%. These results confirmed that the hydrogel scaffold alone did not support cell viability, but when modified with cell-adhesive ligands, promoted an environment sufficient to sustain high cell viability. This result was not surprising, because PC12 cells are inherently poorly adhesive, requiring adhesion promoting proteins to proliferate on substrates and PEG on the other hand, is known to prevent protein and cell binding.<sup>38</sup> In agreement with our findings, adhesion signaling was suggested as a parameter of utmost importance for the survival of primary neural cells<sup>39</sup> and PC12 cells in particular had been shown to attach to RGDS, IKVAV, and YIGSR modified PEG, but not on RGD modified PEG.<sup>36</sup> Additionally, other researchers have shown that primary neural cells, which are also anchorage dependent, adhere preferentially to IKVAV, RGD, or YIGSR modified glass surfaces over PEG modified glass surfaces.<sup>40</sup>

The concentration of adhesive ligands bound to a non-adhesive substrate is also known to strongly affect cell behavior.<sup>36, 41–43</sup> Thus we expected that ligand concentration would further influence PC12 cell viability in our system. Cell viability was determined to be dose dependent, with the lowest cell viability (84%) associated with the lowest concentration of RGDS (2.5  $\mu\text{M}$ ) (Fig. 2b). Optimal conditions were achieved at 50  $\mu\text{M}$  RGDS where cell viability reached 94% and further increases in ligand concentration (100 and 1000  $\mu\text{M}$ ) did not provide further improvement in cell viability. A threshold of RGDS concentration for enhancement of cell attachment, viability, and proliferation had been demonstrated previously. For example, when studying osteoblast proliferation in RGDS-modified PEG copolymer, Behravesh et. al. pinpointed 100  $\mu\text{M}$  RGDS to be optimal with no further improvement in cell proliferation for higher ligand concentrations.<sup>44</sup>

### Effect of hydrogel structure on PC12 cell viability

We have previously reported that cross-linker molecular weight has a negligible effect on the initial hydrogel properties, but strongly influences hydrogel degradation rate and therefore the rate at which the hydrogel physical properties change.<sup>16</sup> Presently, we found that PC12 cell viability was not influenced by the molecular weight of cross-linker used to synthesize the hydrogels (Fig. 3a): cell viability was retained >90% for all cross-linker molecular weights. At 24 h, hydrogel degradation was negligible, thus it is reasonable to expect that the physical properties of the hydrogels examined herein were not significantly different at this time point.

To test the feasibility of encapsulating cells in hydrogels that degrade very quickly (~ hrs for the hydrogels alone and 2–3 days with encapsulated cells), we also tested hydrogels synthesized with PEG-SH 1 3.4 cross-linker. At 24 h, >90% of encapsulated cells were viable (Fig. 3a).

Polymer density, however, had a significant effect on PC12 cell viability after 24 h of encapsulation (Fig. 3b). We observed that both 5% and 10% w/v hydrogels were associated with 94% cell viability, whereas the cell viability decreased to 92% and 84% when the polymer density was increased to 15% and 20%, respectively. Note that the ligand concentration was kept constant for all polymer densities. Other researchers have also reported a decrease in initial cell viability (~20% for osteoblasts at 24 h after seeding) in similar RGD-modified PEG-diacrylate (PEGDA) hydrogels when the polymer density was increased from 10% to 20% w/v.<sup>45</sup> The authors attributed the decrease in cell viability in part to the highly cross-linked network which could lead to transport limitations of nutrients to the encapsulated cells. Yet, it is well understood that cross-link density results not only in tighter mesh size and swelling ratio, which in turn may affect the transport of nutrients, but also in increased matrix stiffness. To estimate the relative contribution of both mesh size (aka swelling ratio) and stiffness on the cell viability, we summarized the hydrogel scaffold properties resulting from the different polymer densities (Table 1). These properties are reported in the absence of cells and therefore not influenced by the cell number. We noted a large decrease in swelling ratio and mesh size associated with the change in polymer density from 5% to 10% w/v. However, no effect stemming from the difference in properties between these hydrogels (5% and 10% w/v polymer density) on cell viability is apparent on Fig. 3b. The largest drop in cell viability was observed between 15% and 20% w/v polymer density hydrogels, a range in which no significant change in swelling ratio or mesh size was noted. Therefore, we deduced that changes in swelling ratio and mesh size within the range examined in this work did not have a significant effect on PC12 cell viability.

In contrast, hydrogel stiffness, represented by shear modulus, could have impacted the viability of the encapsulated PC12 cells. In comparison to the 10% w/v hydrogels, shear modulus increased 2-fold for the 15% w/v hydrogels and 3-fold for the 20% w/v hydrogels. Above a threshold shear modulus ( $> 3 \times 10^3$  Pa), PC12 cell viability progressively decreased. This finding is potentially significant, because we targeted hydrogel shear modulus values to mimic that of soft nervous tissue ( $\sim 10^2 - 10^3$  Pa),<sup>46</sup> but multiple groups have linked the extent of neurite outgrowth to a broader range of material stiffness ( $\sim 1 - 10^5$  Pa) without addressing cell viability.<sup>22, 28, 36, 47-49</sup> Recently, multiple groups have also shown that stiffness affects neural stem cell differentiation.<sup>27, 50</sup> More specifically, using a library of PEG-poly(L-lysine) (PLL) composites, Hynes et. al demonstrated that stiffness directs neural stem cell (NSC) migration and differentiation towards the neuronal lineage and that the modulus primarily associated with this behavior is on the order of brain tissue<sup>9</sup> and Georges et. al demonstrated that matrix stiffness comparable to that of brain tissue selects neuronal over glial growth.<sup>28</sup> Our findings suggest that neuronal viability could be affected within a relatively small range of material shear modulus and therefore should be considered when encapsulating neurons in 3D materials.

### Effect of cell density on PC12 cell viability

Cell density affects cell behavior in a variety of ways, through direct cell-cell contact or through modulation of the cells' immediate environment by altering its mechanics or content of soluble factors and extracellular matrix components.<sup>51, 52</sup> Specifically, PC12 seeding density had been shown to affect enzyme mRNA levels as well as the effect of NGF on the cells.<sup>53</sup> In hepatocytes, it has been shown that cell seeding density below a threshold, reduces the resulting cell viability by 33%.<sup>54</sup> In this work, we tested a wide range of cell concentrations (40,000 to 400,000 cells/ml of hydrogel) but did not detect differences in the cell viability as a function of cell concentration (Fig. 4) indicating that cell viability as a function of cell density is possibly cell- and material-specific. Though the cell density range examined in this study was broad and relevant for cell delivery applications (current NPC delivery studies have been conducted with  $\sim 100,000$  cells of which only a small percentage

survive<sup>55, 56</sup>), we anticipate that a higher threshold in cell density exists wherein viability becomes compromised.

### PC12 cell viability during hydrogel degradation

For the aforementioned studies, we focused on examining cell viability after 24 h of encapsulation because initial cell viability is an important measure of acute toxicity and a relatively quick read-out of the influence of material properties on cell behavior. But to be practical for implantation it is important that the cells retain high viability until released from the hydrogel scaffold. In a 3D scaffold, cell death is usually associated with low diffusivity of oxygen, nutrients and growth factors throughout the material. In a degradable material, such as the hydrogels described herein, the transport of soluble molecules is aided by a progressive increase in scaffold mesh size due to degradation. Based on our previous work,<sup>57</sup> we did not expect diffusion of oxygen, nutrients or NGF to be a limiting factor for cell survival. Furthermore, high neural cell viability retained over extended periods of cell culture, had been shown for PEG hydrogels with similar mesh sizes.<sup>7</sup> In our studies we also observed that PC12 cell viability remained high for at least 72 h of culture (Fig. 5).

We note that both crosslinker type (Fig. 3a) and polymer density (Fig. 3b) affect hydrogel degradation rate, leading to degradation times from hours to days and potentially weeks,<sup>16</sup> which correlates well with *in-vivo* NPCs transplantation requirements.<sup>58</sup> In particular, necrosis is greatest up to 24 h post-transplantation,<sup>59</sup> while cell death via apoptosis could peak at several days to a week post-transplantation.<sup>60</sup> However, the exact rate of hydrogel degradation and cell delivery required for complete structural and functional tissue recovery are widely variable and determined by multitude of factors, including cell types involved (transplanted cells as well as host cells), site of implantation, host environment, soluble factors, as well as presence of support cells.

### Cell phenotype following release from the hydrogel scaffolds

The ultimate goal of this work was to identify hydrogel scaffold properties that significantly alter cell viability as well as cell phenotype following release from the hydrogel. We selected a hydrogel system (PEG-SH 1 3.4 cross-linker, which was chosen for its fast degradation, 10% w/v total polymer density, 100  $\mu$ M ligand, and 50 ng/ml NGF) that allowed high PC12 cell viability during cell encapsulation and hydrogel degradation. We selected three ligand types, RGDS, IKVAV, and YIGSR, to represent the cell adhesion domains of three extracellular matrix molecules relevant to neural tissue engineering, collagen, fibronectin, and laminin. We hypothesized that the presence of these ligands during encapsulation may differentially influence the ultimate fate of PC12 cells following their release from the degraded hydrogel. Note that the focus of the present work is not on the effect of the adhesive ligand on hydrogel-encapsulated cells, but rather the effect of the adhesive ligand on the cells after release from the hydrogel and subsequent spreading on the collagen coated glass coverslips.

The importance of scaffold-mediated biological signals in guiding stem cell response has long been recognized. In particular, the type and density of the cell binding domain has been shown to strongly affect stem cell differentiation.<sup>43, 61</sup> For example, in the absence of a binding domain, such as in unmodified PEG, NPCs differentiated into neurons and glia with a large glial population which may be undesirable for most applications.<sup>7</sup> In contrast, NSCs, which exhibited poor differentiation on unmodified PEG hydrogels, differentiated primarily into neurons on RGD-modified hydrogels.<sup>10</sup> PC12 cells have also been shown to differentiate into the neuronal phenotype and extend a greater number of long neurites in RGD-containing hydrogels compared to hydrogels containing the non-functional RDG peptide sequence.<sup>62</sup> Furthermore, nanofibers composed of IKVAV ligand have been shown



to promote neuronal differentiation of NSCs and to decrease astrocytic differentiation relative to the native laminin.<sup>63</sup> Thus, we hypothesized that incorporation of adhesive ligand sequences would not only promote PC12 cell viability but would affect the PC12 cell fate upon delivery and potentially, would have an impact in future studies of this material with encapsulated NPCs.

We observed that all hydrogel scaffolds, containing RGDS, IKVAV or YIGSR, were able to release PC12 cells expressing the neuronal phenotype (Fig. 6) with comparable neurite length distributions (Fig. 7). The peak frequency for all hydrogel types was at neurite length of 20–30  $\mu\text{m}$ . The longest neurites were 150  $\mu\text{m}$  (normalized frequency of 2.5), 240  $\mu\text{m}$  (normalized frequency of 0.6), and 370  $\mu\text{m}$  (normalized frequency of 0.3), for RGDS, IKVAV and YIGSR, respectively.

Cells released from hydrogels containing RGDS or YIGSR, typically had an elongated shape with thin filopodia, whereas cells released from hydrogels containing IKVAV, were more spread and had tubulin-rich lamellipodia and fewer filopodia. However, quantitative image analysis of the percent of cells extending neurites (Fig. 7c) revealed that cells released from hydrogels containing RGDS and IKVAV had a ~2-fold greater percentage of cells with neurites compared to cells released from the YIGSR hydrogels. Gunn and Mann<sup>36</sup> cultured PC12 cells on top of PEG-dimethacrylate hydrogels that were modified with the same ligands investigated herein; they found that the PC12 cells extended neurites on the RGDS- and IKVAV-modified hydrogels but not the YIGSR-modified hydrogels. This result agrees with our findings that the presence of YIGSR in the hydrogel system was not as effective at promoting neurite outgrowth as compared to RGDS and IKVAV. However, Gunn and Mann cultured the cells on top of the ligand-modified hydrogels so that the PC12 cells were in direct contact with the insoluble ligand throughout the experiment. Our results suggest that the effect of YIGSR persisted following complete hydrogel degradation, indicating that this response may not be exclusively reliant on cell binding to insoluble YIGSR or that the effect of the cells' interaction with insoluble YIGSR early in the culture period was significant enough to influence cellular response for several days following hydrogel degradation.

Aside from the possible direct influence of YIGSR on the PC12 cell fate, due to specific biological interactions, the ligand could be influencing the cell fate indirectly via its effect on hydrogel properties. In our previous work, we demonstrated that specific ligands can significantly alter hydrogel properties.<sup>15</sup> As mentioned earlier in the discussion, hydrogels containing encapsulated cells degraded slower than cell-free hydrogels, but YIGSR-modified hydrogels containing cells took approximately twice as long to degrade completely as compared to RGDS- and IKVAV-modified hydrogels (~6 d vs ~3–4 d, respectively). Additionally, the effect of ligand on hydrogel swelling and shear modulus was most pronounced for hydrogels containing YIGSR, namely, it lead to decrease in swelling ratio and mesh size and increase in storage modulus.<sup>15</sup> The decrease in swelling ratio in the presence of YIGSR (compared to hydrogels with no ligand or to RGDS- and IKVAV-modified hydrogels) may explain the slower hydrogel degradation. However, additional studies would be necessary to investigate if altered hydrogel mechanical or biochemical properties in the presence of the YIGSR ligand are responsible for the lower number of PC12 cells expressing neurites. Overall, we saw that the mechanical and biological environment may influence not only the initial cell response but even provide a 'pre-conditioning' effect that may persist for several days following hydrogel degradation.

An alternative explanation for the lower percentage of cells extending neurites in YIGSR-modified hydrogels is the slower degradation of these hydrogels compared to the RGDS- and IKVAV-modified hydrogels. To test if this could be an underlying reason and to confirm that PC12 cells would still express the neural phenotype when encapsulated for

longer periods of time, we tested cell response following release from PEG hydrogels made with PEG-SH 2 3.4 cross-linker, which degraded in 10–14 days in the presence of cells (data not shown). There was no significant difference in the number of cells extending neurites or the neurite length distribution between hydrogels made with PEG-SH 1 3.4 or PEG-SH 2 3.4 cross-linkers, for any one ligand type (RGDS, IKVAV, or YIGSR). From these results, we inferred the following: first, the difference in the percent of cells released from YIGSR-modified hydrogels that extend neurites was not due to slower hydrogel degradation; and second, even upon culture for up to 2 weeks, the degradable hydrogels were able to deliver PC12 cells capable of expressing the neuronal phenotype. Therefore, degradation time and consequently the timing of cell release can be controlled by varying the hydrogel composition (via cross-linker type or molecular weight) without compromising cell viability or differentiation. The versatility of this system renders it useful both in applications where rapid cell delivery or prolonged cell encapsulation may be required.

## Conclusions

We conclude that the hydrolytically degradable PEG hydrogel scaffold recently reported by our laboratory was capable of supporting high cell viability as well as PC12 cell differentiation to the neuronal phenotype. To our knowledge, aside from PEG copolymers,<sup>7, 8, 64</sup> this is the first hydrogel composed PEG alone that has been reported for the delivery of neural-like cells. The major advantage of the developed scaffold, as described in detail in our previous publication,<sup>16</sup> was that it allowed for modulation of stiffness, adhesivity and degradability and thus permitted the delineation of the various factors contributing to the complexity of the hydrogel scaffold. In context of the current work, we pinpointed the effect of several key mechanical and biological properties of the scaffold on cell viability and the role of ligand type on the resulting cell phenotype following release from the hydrogel. For example, we demonstrated that polymer density and adhesive ligand concentration had the most pronounced effect on PC12 cell viability. Summarizing the hydrogel properties as a function of polymer density, we were able to link the decrease in cell viability to increase in the storage modulus of the hydrogel. Additionally, we demonstrated that PC12 cell fate can be controlled by the addition of biochemical cues, such as adhesive ligands, to the hydrogel. We further illustrated that PC12 cells express the neuronal phenotype even after prolonged encapsulation time and that the timing of the cell release can be controlled by the type of cross-linker. Thus, this work lays the groundwork for application of this hydrogel system towards encapsulation of NPCs and optimization of their differentiation towards a specific neuronal or glial cell fate.

## Acknowledgments

We thank Shelby Vargo and Helena Gaifem for assistance with studies. This work was supported by NIH-NINDS (R01NS065205), the Henry Luce Foundation, and a UMBC-Wyeth Fellowship to Andreia Ribeiro.

## References

1. Piccini P, Pavese N, Hagell P, Reimer J, Bjorklund A, Oertel WH, Quinn NP, Brooks DJ, Lindvall O. Factors affecting the clinical outcome after neural transplantation in Parkinson's disease. *Brain*. 2005; 128:2977–2986. [PubMed: 16246865]
2. Lepore AC, Neuhuber B, Connors TM, Han SS, Liu Y, Daniels MP, Rao MS, Fischer I. Long-term fate of neural precursor cells following transplantation into developing and adult CNS. *Neuroscience*. 2006; 142:287–304. [PubMed: 17120358]
3. Emsley JG, Mitchell BD, Kempermann G, Macklis JD. Adult neurogenesis and repair of the adult CNS with neural progenitors, precursors, and stem cells. *Prog Neurobiol*. 2005; 75:321–341. [PubMed: 15913880]

4. An Y, Tsang KK, Zhang H. Potential of stem cell based therapy and tissue engineering in the regeneration of the central nervous system. *Biomed Mater.* 2006; 1:R38–R44. [PubMed: 18460755]
5. Schmidt CE, Leach JB. Neural tissue engineering: strategies for repair and regeneration. *Annu Rev Biomed Eng.* 2003; 5:293–347. [PubMed: 14527315]
6. Straley KS, Foo CW, Heilshorn SC. Biomaterial design strategies for the treatment of spinal cord injuries. *J Neurotrauma.* 2010; 27:1–19. [PubMed: 19698073]
7. Mahoney MJ, Anseth KS. Three-dimensional growth and function of neural tissue in degradable polyethylene glycol hydrogels. *Biomaterials.* 2006; 27:2265–2274. [PubMed: 16318872]
8. Hynes SR, McGregor LM, Millicent FR, Lavik EB. Photopolymerized poly(ethylene glycol)/poly(L-lysine) hydrogels for the delivery of neural progenitor cells. *Journal of Biomaterials Science, Polymer Edition.* 2007; 18:1017–1030. [PubMed: 17705996]
9. Hynes SR, Rauch MF, Bertram JP, Lavik EB. A library of tunable poly(ethylene glycol)/poly(L-lysine) hydrogels to investigate the material cues that influence neural stem cell differentiation. *J Biomed Mater Res A.* 2009; 89:499–509. [PubMed: 18435406]
10. Freudenberg U, Hermann A, Welzel PB, Stirl K, Schwarz SC, Grimmer M, Zieris A, Panyanuwat W, Zschoche S, Meinhold D, Storch A, Werner C. A star-PEG-heparin hydrogel platform to aid cell replacement therapies for neurodegenerative diseases. *Biomaterials.* 2009; 30:5049–5060. [PubMed: 19560816]
11. Miller K, Chinzei K, Orssengo G, Bednarz P. Mechanical properties of brain tissue in-vivo: experiment and computer simulation. *J Biomech.* 2000; 33:1369–1376. [PubMed: 10940395]
12. Wilson JT, Chaikof EL. Challenges and emerging technologies in the immunoisolation of cells and tissues. *Adv Drug Deliv Rev.* 2008; 60:124–145. [PubMed: 18022728]
13. Modo M, Rezaie P, Heuschling P, Patel S, Male DK, Hodges H. Transplantation of neural stem cells in a rat model of stroke: assessment of short-term graft survival and acute host immunological response. *Brain Res.* 2002; 958:70–82. [PubMed: 12468031]
14. Sawhney AS, Pathak CP, A HJ. Bioerodible hydrogels based on photopolymerized poly(ethylene glycol)-co-poly(.alpha.-hydroxy acid) diacrylate macromers. *Macromolecules.* 1993; 26:581–587.
15. Zustiak SP, Durbal R, Leach JB. Influence of cell-adhesive peptide ligands on poly(ethylene glycol) hydrogel physical, mechanical and transport properties. *Acta Biomater.* 2010
16. Zustiak SP, Leach JB. Hydrolytically degradable poly(ethylene glycol) hydrogel scaffolds with tunable degradation and mechanical properties. *Biomacromolecules.* 2010; 11:1348–1357. [PubMed: 20355705]
17. Greene LA, Tischler AS. Establishment of a noradrenergic clonal line of rat adrenal pheochromocytoma cells which respond to nerve growth factor. *Proc Natl Acad Sci U S A.* 1976; 73:2424–2428. [PubMed: 1065897]
18. Tomaselli KJ, Damsky CH, Reichardt LF. Interactions of a neuronal cell line (PC12) with laminin, collagen IV, fibronectin: identification of integrin-related glycoproteins involved in attachment and process outgrowth. *J Cell Biol.* 1987; 105:2347–2358. [PubMed: 3500175]
19. Yu X, Dillon GP, Bellamkonda RB. A laminin and nerve growth factor-laden three-dimensional scaffold for enhanced neurite extension. *Tissue Eng.* 1999; 5:291–304. [PubMed: 10477852]
20. Lutolf MP, Lauer-Fields JL, Schmoekel HG, Metters AT, Weber FE, Fields GB, Hubbell JA. Synthetic matrix metalloproteinase-sensitive hydrogels for the conduction of tissue regeneration: engineering cell-invasion characteristics. *Proc Natl Acad Sci U S A.* 2003; 100:5413–5418. [PubMed: 12686696]
21. Lutolf MP, Tirelli N, Cerritelli S, Cavalli L, Hubbell JA. Systematic modulation of Michael-type reactivity of thiols through the use of charged amino acids. *Bioconjug Chem.* 2001; 12:1051–1056. [PubMed: 11716699]
22. Leach JB, Brown XQ, Jacot JG, Dimilla PA, Wong JY. Neurite outgrowth and branching of PC12 cells on very soft substrates sharply decreases below a threshold of substrate rigidity. *J Neural Eng.* 2007; 4:26–34. [PubMed: 17409477]
23. Saha K, Pollock JF, Schaffer DV, Healy KE. Designing synthetic materials to control stem cell phenotype. *Curr Opin Chem Biol.* 2007; 11:381–387. [PubMed: 17669680]
24. Hwang NS, Varghese S, Elisseeff J. Controlled differentiation of stem cells. *Adv Drug Deliv Rev.* 2008; 60:199–214. [PubMed: 18006108]

25. Teixeira AI, Duckworth JK, Hermanson O. Getting the right stuff: controlling neural stem cell state and fate in vivo and in vitro with biomaterials. *Cell Res.* 2007; 17:56–61. [PubMed: 17211445]
26. Thonhoff JR, Lou DI, Jordan PM, Zhao X, Wu P. Compatibility of human fetal neural stem cells with hydrogel biomaterials in vitro. *Brain Res.* 2008; 1187:42–51. [PubMed: 18021754]
27. Banerjee A, Arha M, Choudhary S, Ashton RS, Bhatia SR, Schaffer DV, Kane RS. The influence of hydrogel modulus on the proliferation and differentiation of encapsulated neural stem cells. *Biomaterials.* 2009; 30:4695–4699. [PubMed: 19539367]
28. Georges PC, Miller WJ, Meaney DF, Sawyer E, Janmey PA. Matrices with compliance comparable to that of brain tissue select neuronal over glial growth in mixed cortical cultures. *Biophys J.* 2006; 90:3012–3018. [PubMed: 16461391]
29. Seidlits SK, Khaing ZZ, Petersen RR, Nickels JD, Vanscoy JE, Shear JB, Schmidt CE. The effects of hyaluronic acid hydrogels with tunable mechanical properties on neural progenitor cell differentiation. *Biomaterials.* 2010; 31:3930–3940. [PubMed: 20171731]
30. Young TH, Huang JH, Hung SH, Hsu JP. The role of cell density in the survival of cultured cerebellar granule neurons. *J Biomed Mater Res.* 2000; 52:748–753. [PubMed: 11033558]
31. Brannvall K, Bergman K, Wallenquist U, Svahn S, Bowden T, Hilborn J, Forsberg-Nilsson K. Enhanced neuronal differentiation in a three-dimensional collagen-hyaluronan matrix. *J Neurosci Res.* 2007; 85:2138–2146. [PubMed: 17520747]
32. Bryant SJ, Durand KL, Anseth KS. Manipulations in hydrogel chemistry control photoencapsulated chondrocyte behavior and their extracellular matrix production. *J Biomed Mater Res A.* 2003; 67:1430–1436. [PubMed: 14624532]
33. Cukierman E, Pankov R, Stevens DR, Yamada KM. Taking cell-matrix adhesions to the third dimension. *Science.* 2001; 294:1708–1712. [PubMed: 11721053]
34. Lutolf MP, Raeber GP, Zisch AH, Tirelli N, Hubbell JA. Cell-Responsive Synthetic Hydrogels. *Advanced Materials.* 2003; 15:888–892.
35. Bryant SJ, Chowdhury TT, Lee DA, Bader DL, Anseth KS. Crosslinking density influences chondrocyte metabolism in dynamically loaded photocrosslinked poly(ethylene glycol) hydrogels. *Ann Biomed Eng.* 2004; 32:407–417. [PubMed: 15095815]
36. Gunn JW, Turner SD, Mann BK. Adhesive and mechanical properties of hydrogels influence neurite extension. *J Biomed Mater Res A.* 2005; 72:91–97. [PubMed: 15536643]
37. Park KH, Yun K. Immobilization of Arg-Gly-Asp (RGD) sequence in a thermosensitive hydrogel for cell delivery using pheochromocytoma cells (PC12). *J Biosci Bioeng.* 2004; 97:374–377. [PubMed: 16233645]
38. Franks W, Tosatti S, Heer F, Seif P, Textor M, Hierlemann A. Patterned cell adhesion by self-assembled structures for use with a CMOS cell-based biosensor. *Biosens Bioelectron.* 2007; 22:1426–1433. [PubMed: 17055243]
39. Nakaji-Hirabayashi T, Kato K, Iwata H. Self-assembling chimeric protein for the construction of biodegradable hydrogels capable of interaction with integrins expressed on neural stem/progenitor cells. *Biomacromolecules.* 2008; 9:1411–1416. [PubMed: 18429629]
40. Saneinejad S, Shoichet MS. Patterned glass surfaces direct cell adhesion and process outgrowth of primary neurons of the central nervous system. *J Biomed Mater Res.* 1998; 42:13–19. [PubMed: 9740002]
41. Kraehenbuehl T, Zammaretti P, Van der Vlies A, Schoenmakers R, Lutolf M, Jaconi M, Hubbell J. Three-dimensional extracellular matrix-directed cardioprogenitor differentiation: systematic modulation of a synthetic cell-responsive PEG-hydrogel. *Biomaterials.* 2008; 29:2757–2766. [PubMed: 18396331]
42. Schense JC, Bloch J, Aebischer P, Hubbell JA. Enzymatic incorporation of bioactive peptides into fibrin matrices enhances neurite extension. *Nat Biotechnol.* 2000; 18:415–419. [PubMed: 10748522]
43. Pittier R, Sauthier F, Hubbell JA HH. Neurite extension and in vitro myelination within three-dimensional modified fibrin matrices. *Journal of Neurobiology.* 2005; 63:1–14. [PubMed: 15616962]

44. Behravesh E, Zygourakis K, Mikos AG. Adhesion and migration of marrow-derived osteoblasts on injectable in situ crosslinkable poly(propylene fumarate-co-ethylene glycol)-based hydrogels with a covalently linked RGDS peptide. *J Biomed Mater Res A*. 2003; 65:260–270. [PubMed: 12734821]
45. Burdick JA, Anseth KS. Photoencapsulation of osteoblasts in injectable RGD-modified PEG hydrogels for bone tissue engineering. *Biomaterials*. 2002; 23:4315–4323. [PubMed: 12219821]
46. Lu YB, Franze K, Seifert G, Steinhauser C, Kirchhoff F, Wolburg H, Guck J, Janmey P, Wei EQ, Kas J, Reichenbach A. Viscoelastic properties of individual glial cells and neurons in the CNS. *Proc Natl Acad Sci U S A*. 2006; 103:17759–17764. [PubMed: 17093050]
47. Willits RK, Skornia SL. Effect of collagen gel stiffness on neurite extension. *J Biomat Sci, Polymer Ed*. 2004; 15:1521–1531.
48. Balgude AP, Yu X, Szymanski A, Bellamkonda RV. Agarose gel stiffness determines rate of DRG neurite extension in 3D cultures. *Biomaterials*. 2001; 22:1077–1084. [PubMed: 11352088]
49. Flanagan LA, Ju YE, Marg B, Osterfield M, Janmey PA. Neurite branching on deformable substrates. *Neuroreport*. 2002; 13:2411–2415. [PubMed: 12499839]
50. Saha K, Keung AJ, Irwin EF, Li Y, Little L, Schaffer DV, Healy KE. Substrate modulus directs neural stem cell behavior. *Biophys J*. 2008; 95:4426–4438. [PubMed: 18658232]
51. Shapira-Schweitzer K, Seliktar D. Matrix stiffness affects spontaneous contraction of cardiomyocytes cultured within a PEGylated fibrinogen biomaterial. *Acta Biomater*. 2007; 3:33–41. [PubMed: 17098488]
52. Warchol ME. Cell density and N-cadherin interactions regulate cell proliferation in the sensory epithelia of the inner ear. *J Neurosci*. 2002; 22:2607–2616. [PubMed: 11923426]
53. Badoyannis HC, Sharma SC, Sabban EL. The differential effects of cell density and NGF on the expression of tyrosine hydroxylase and dopamine beta-hydroxylase in PC12 cells. *Brain Res Mol Brain Res*. 1991; 11:79–87. [PubMed: 1685006]
54. Dvir-Ginzberg M, Gamlieli-Bonshtein I, Agbaria R, Cohen S. Liver Tissue Engineering within Alginate Scaffolds: Effects of Cell-Seeding Density on Hepatocyte Viability, Morphology, and Function. *Tissue Engineering*. 2004; 9:757–766. [PubMed: 13678452]
55. Okada S, Ishii K, Yamane J, Iwanami A, Ikegami T, Katoh H, Iwamoto Y, Nakamura M, Miyoshi H, Okano HJ, Contag CH, Toyama Y, Okano H. In vivo imaging of engrafted neural stem cells: its application in evaluating the optimal timing of transplantation for spinal cord injury. *FASEB J*. 2005; 19:1839–1841. [PubMed: 16141363]
56. Shear DA, Tate MC, Archer DR, Hoffman SW, Hulce VD, Laplaca MC, Stein DG. Neural progenitor cell transplants promote long-term functional recovery after traumatic brain injury. *Brain Res*. 2004; 1026:11–22. [PubMed: 15476693]
57. Zustiak SP, Boukari H, Leach JB. Solute diffusion and interactions in cross-linked poly(ethylene glycol) hydrogels studied by fluorescence correlation spectroscopy. *Soft Matter*. 2010; 6:3609–3618.
58. Cooke MJ, Vulic K, Shoichet MS. Design of biomaterials to enhance stem cell survival when transplanted into the damaged central nervous system. *Soft Matter*. 2010; 6:4988–4998.
59. Hill CE, Hurtado A, Blits B, Bahr BA, Wood PM, Bartlett Bunge M, Oudega M. Early necrosis and apoptosis of Schwann cells transplanted into the injured rat spinal cord. *Eur J Neurosci*. 2007; 26:1433–1445. [PubMed: 17880386]
60. Bakshi A, Keck CA, Koshkin VS, LeBold DG, Siman R, Snyder EY, McIntosh TK. Caspase-mediated cell death predominates following engraftment of neural progenitor cells into traumatically injured rat brain. *Brain Res*. 2005; 1065:8–19. [PubMed: 16309635]
61. Battista S, Guarnierib D, Borsellib C, Zeppetellia S, Borzacchielloa A, Mayolb L, Gerbasiod D, Keenec DR, Ambrosioa L, Netti PA. The effect of matrix composition of 3D constructs on embryonic stem cell differentiation. *Biomaterials*. 2005; 26:6194–6207. [PubMed: 15921736]
62. Straley KS, Heilshorn SC. Independent tuning of multiple biomaterial properties using protein engineering. *Soft Matter*. 2009; 5:114–124.
63. Silva GA, Czeisler C, Niece KL, Beniash E, Harrington DA, Kessler JA, Stupp SI. Selective differentiation of neural progenitor cells by high-epitope density nanofibers. *Science*. 2004; 303:1352–1355. [PubMed: 14739465]



64. Namba RM, Cole AA, Bjugstad KB, Mahoney MJ. Development of porous PEG hydrogels that enable efficient, uniform cell-seeding and permit early neural process extension. *Acta Biomaterialia*. 2009; 5:1884–1897. [PubMed: 19250891]

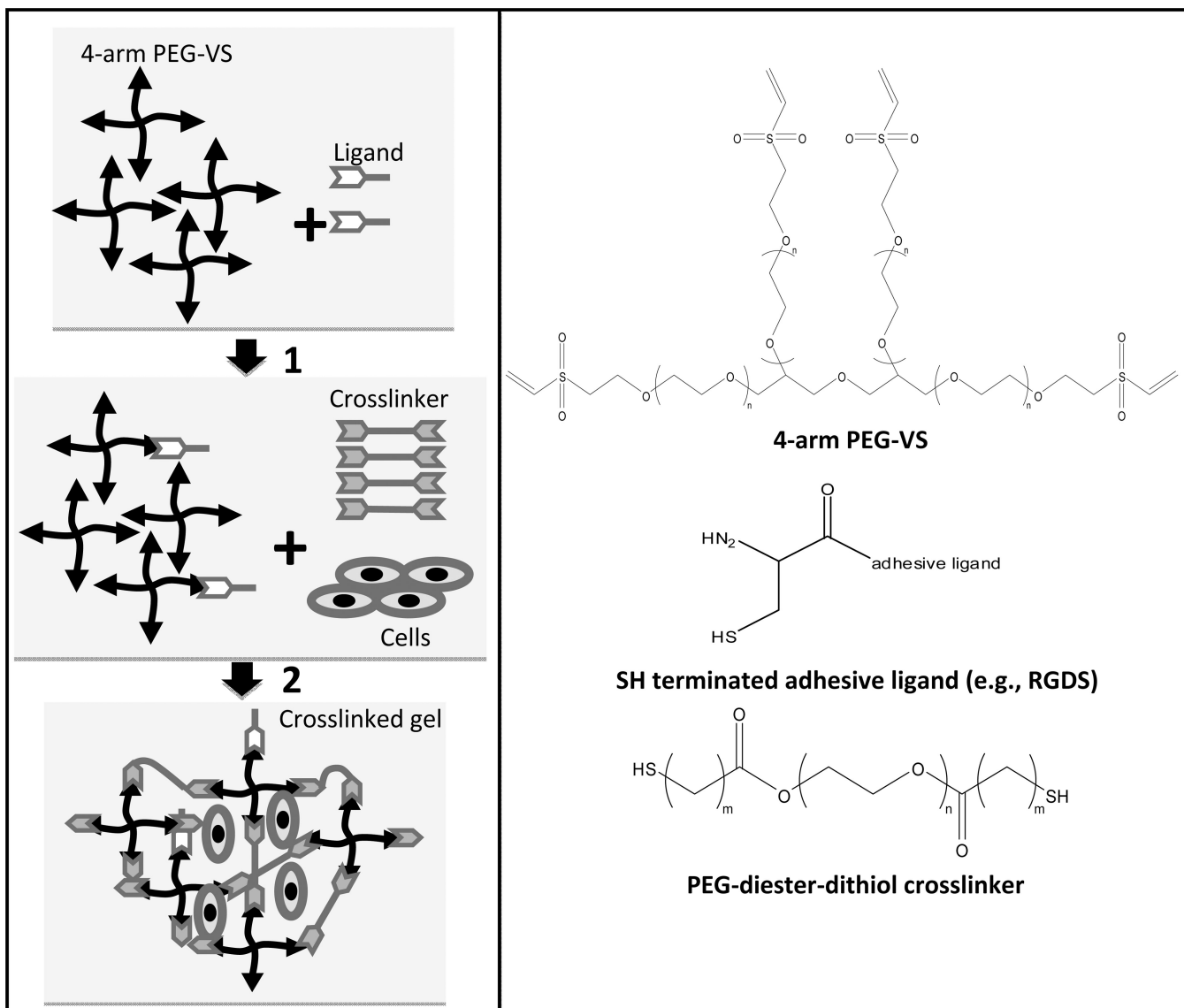


**Figure 1.** Schematic of the hydrogel scaffold cross-linking reaction. To prepare the hydrogels, 4-arm poly(ethylene glycol)-vinyl sulfone (4-arm PEG-VS) was first reacted with a cell adhesive ligand (GRCD- $x$ -PD where  $x$  represents RGDS, IKVAV or YIGSR) at a large stoichiometric deficit of ligand to the reactive groups of 4-arm PEG-VS (ligand cysteine SH  $\ll$  VS). In a second step, hydrolytically degradable cross-linker, PEG-diester-dithiol, was added to bring the total ratio of SH:VS to 1:1. PC12 cells were encapsulated at that time as well. Hydrogel degradation rate can be controlled by altering the number of methylene groups between the cross-linker thiol and ester moieties (indicated by  $m$ ) or cross-linker molecular weight (indicated by  $n$ , the number of  $\text{CH}_2\text{CH}_2\text{O}$  repeats).

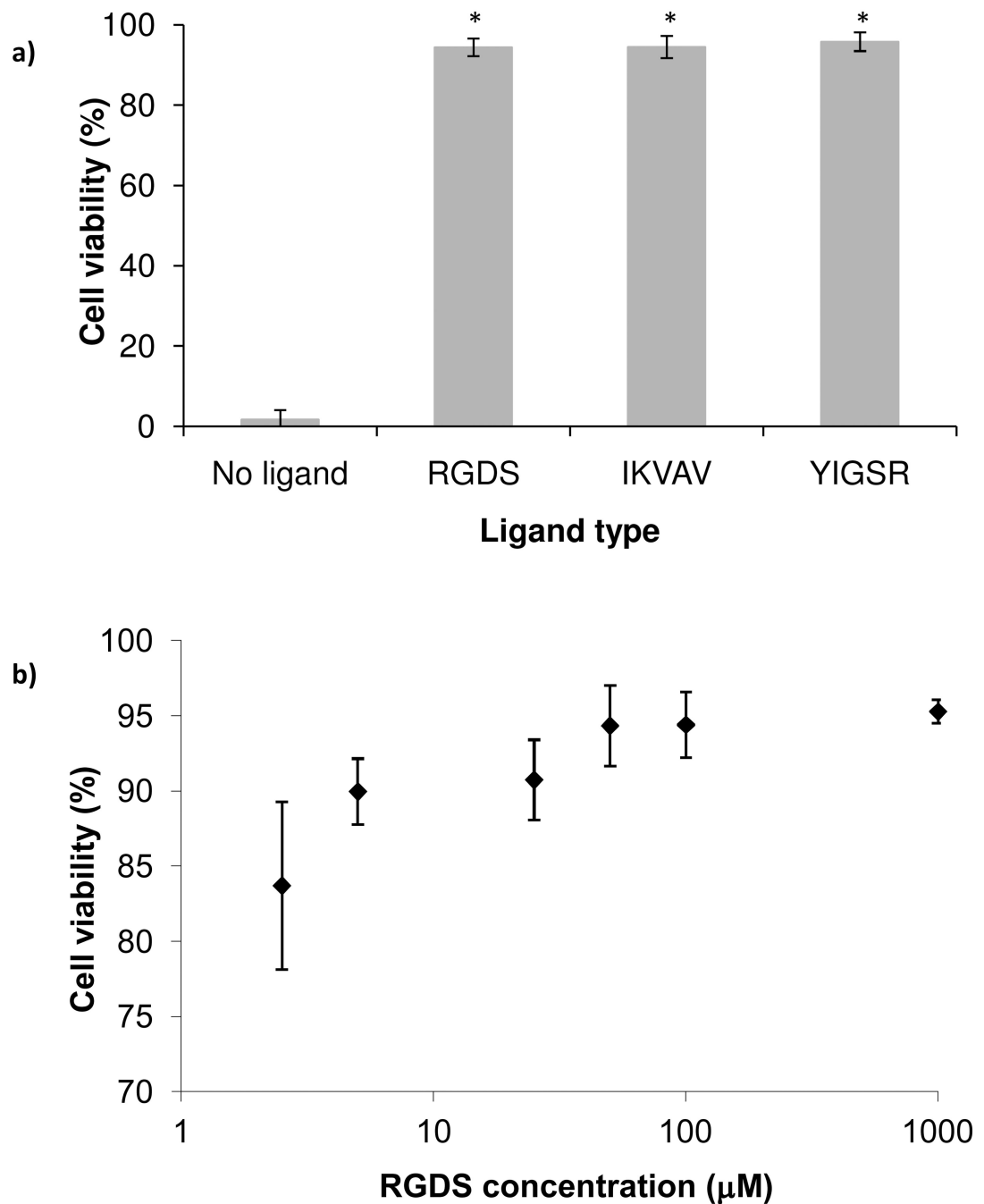


**Figure 2.** PC12 cell viability after 24 h encapsulation in PEG hydrogels with covalently incorporated ligand: effect of ligand type and density. All hydrogels were 10% w/v and synthesized with PEH-SH 2 3.4 cross-linker: (a). PC12 cell viability as a function of ligand type – 100 μM of RGDS, IKVAV or YIGSR. Asterisks designate significant differences from hydrogels without ligand ( $n = 18$ ); (b) PC12 cell viability as a function of RGDS ligand concentration ( $n = 30$ ). Cell viabilities at ligand concentrations of 50 μM and above are significantly different from viabilities at ligand densities of 2.5, 5 and 25 μM.

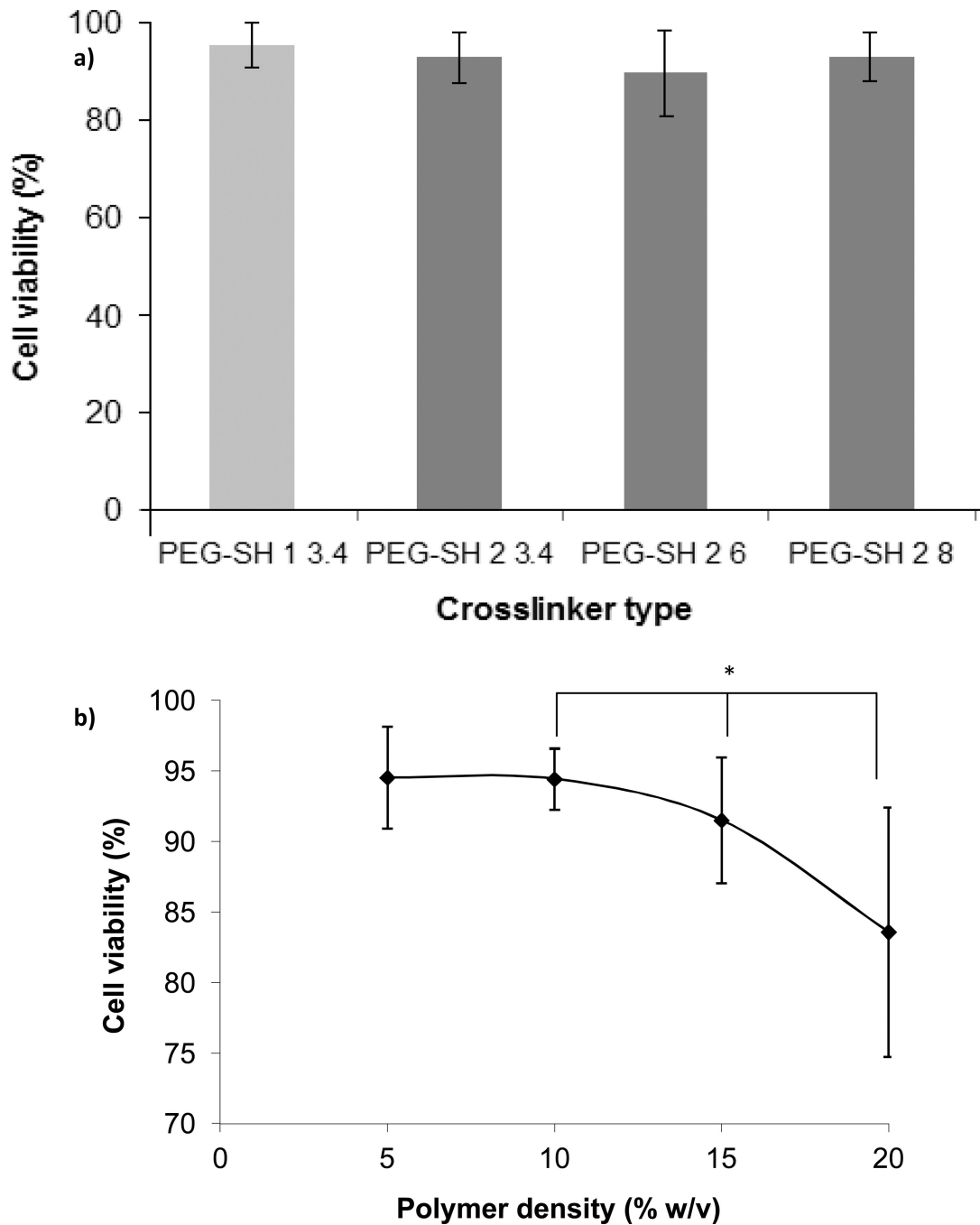


**Figure 3.**

PC12 cell viability after 24 h of encapsulation in PEG hydrogels: effect of hydrogel structure. All hydrogels were 10% w/v in total polymer and contained 100  $\mu$ M RGDS ligand: (a) PC12 cell viability as a function of cross-linker molecular weight and number of methylene groups between the thiol and ester moieties ( $n = 30$ ); (b) PC12 cell viability as a function of hydrogel polymer density ( $n = 18$ ). All hydrogels were synthesized with PEG-SH 2 3.4 cross-linker. Asterisk designates significant differences. The line connecting data points is provided to guide the eye.

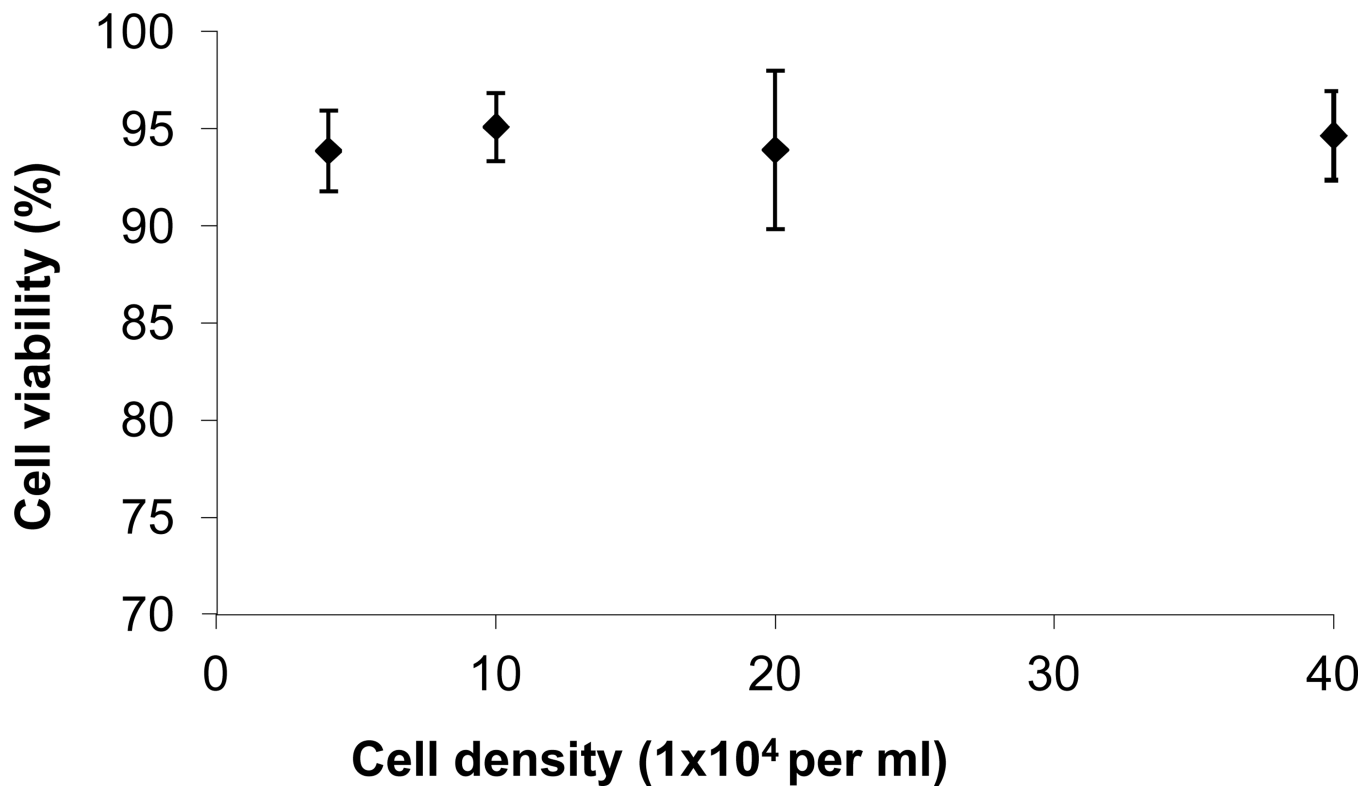


**Figure 4.** PC12 cell viability after 24 h of encapsulation as a function of cell density ( $n = 18$ ). All hydrogels were 20  $\mu$ l, 10% w/v total polymer density and synthesized with PEG-SH 2 3.4 cross-linker and 100  $\mu$ M RGDS ligand.



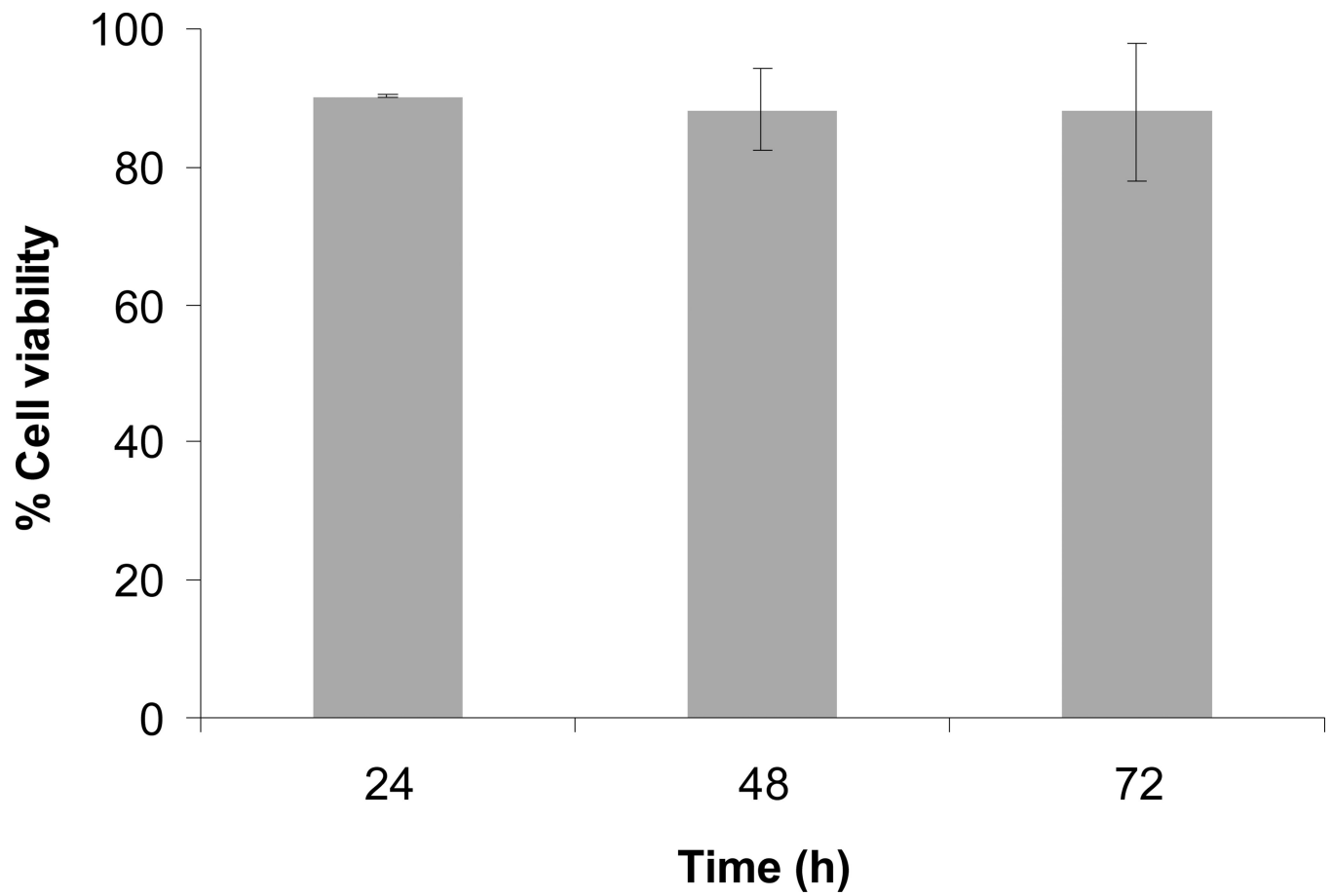


**Figure 5.** PC12 cell viability as a function of culture duration (n = 30). All hydrogels were 10% w/v total polymer density prepared with PEG-SH 2 3.4 cross-linker and 100  $\mu$ M RGDS ligand.

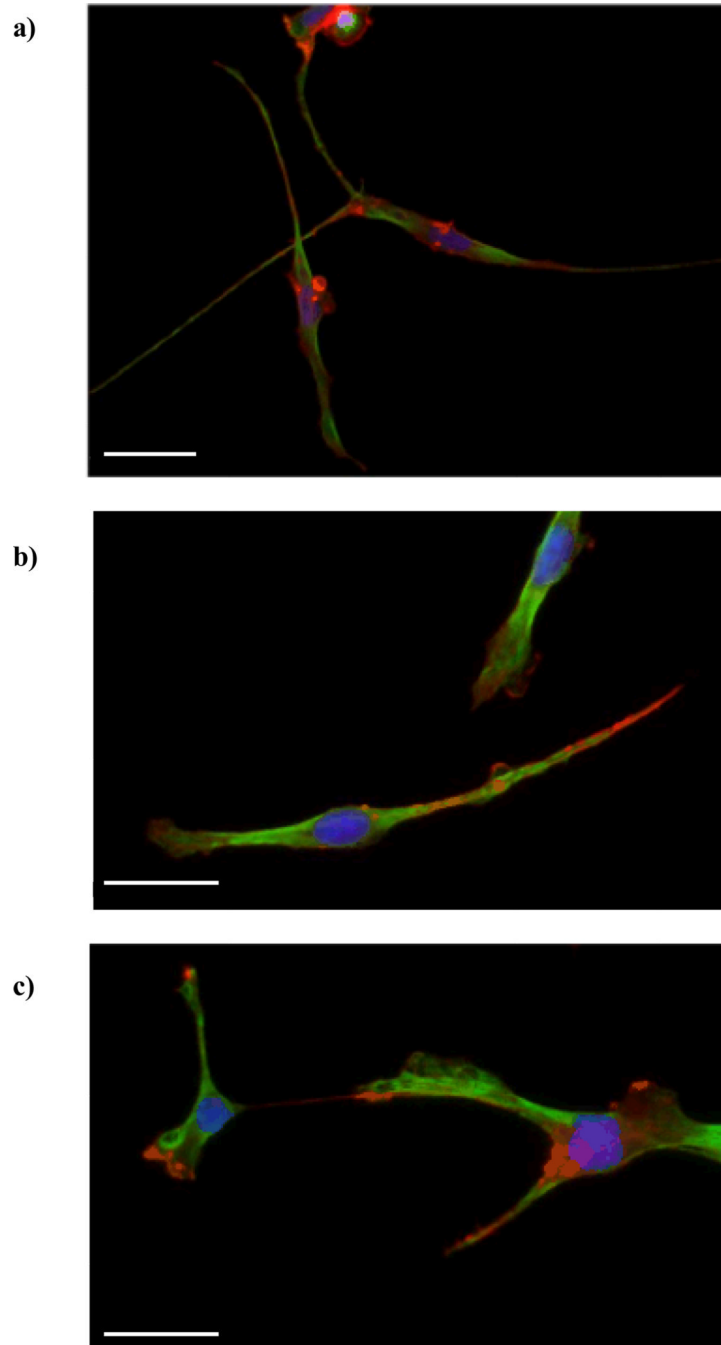


**Figure 6.** Immunofluorescent images of PC12 cells following release from the hydrogel scaffolds. The cells were embedded in PEG hydrogels containing RGDS (a), YIGSR (b), or IKVAV (c) ligands (100  $\mu$ M) and were released upon hydrogel degradation. The cells adhering to the collagen-coated coverslips (placed underneath the hydrogels) were fixed and stained 48 h after hydrogel degradation. Neurons were co-labeled for actin (red) and tubulin (green). Cell nuclei were labeled with DAPI (blue). Scale bars are 50  $\mu$ m.

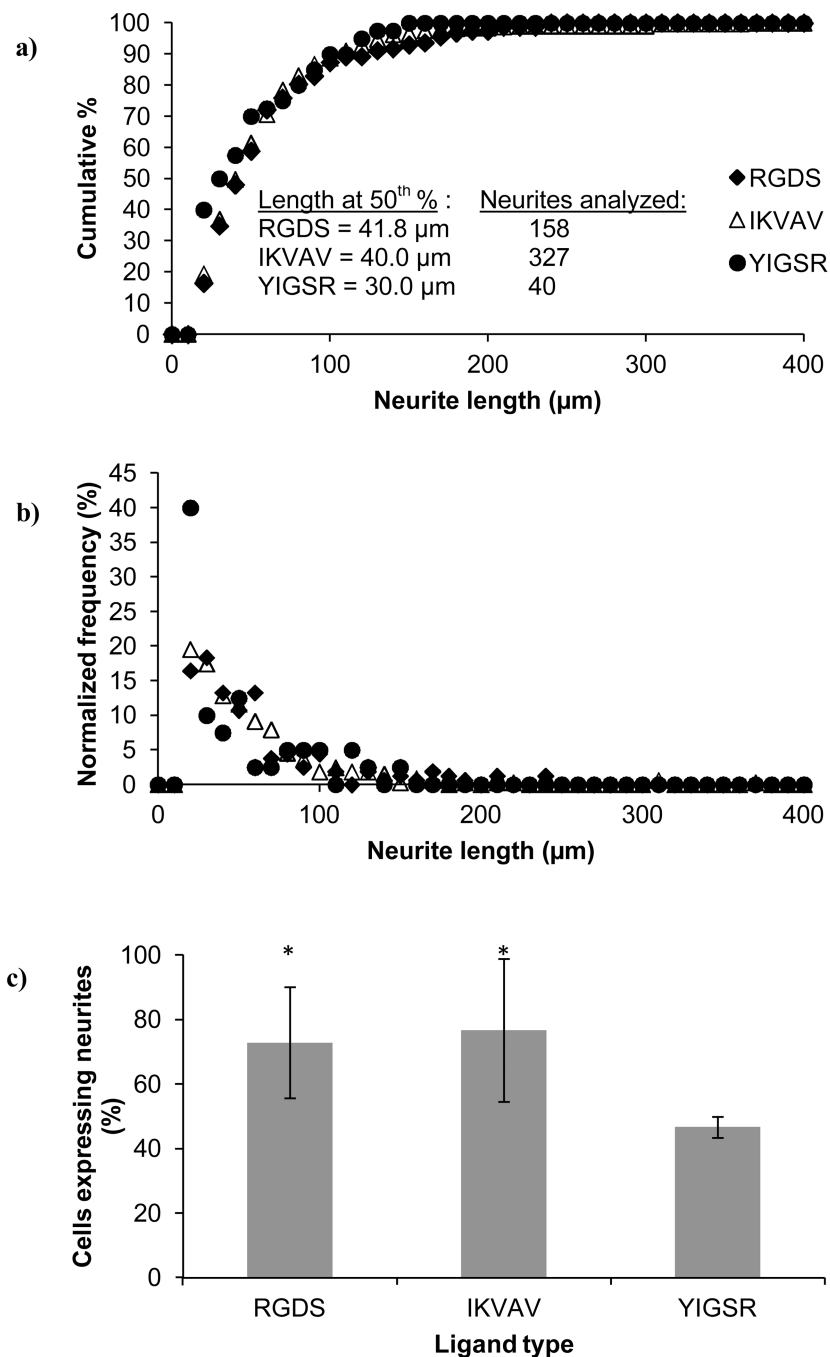


**Figure 7.**

Neurite extension following release from the PEG scaffolds. The cells were embedded in PEG hydrogels containing RGDS, IKVAV or YIGSR ligands (100  $\mu\text{M}$ ) and were released upon hydrogel degradation. Cell analysis were performed 48 h after the cells had been released from the hydrogels and adhered onto collagen-coated coverslips. Neurite length, represented by (a) the cumulative distribution and (b) the normalized frequency, as well as (c) the number of cells with neurites, revealed differences between the PC12 cells released from the YIGSR-modified PEG hydrogels, compared to the RGDS- or IKVAV-modified PEG hydrogels. Asterisks designate significant differences from YIGSR in (c).

**Table 1**

Summary of the PEG hydrogel properties adapted from Zustiak et. al<sup>16</sup>. Conditions for the experiments were as follows: PEG-SH 2 3.4 cross-linker, 10% w/v polymer density, no adhesive ligand present. Swelling ratio was defined as the mass of the swollen hydrogel divided by the mass of the dehydrated hydrogel and was used to calculate mesh size from Flory-Rehner theory. Shear modulus,  $G'$ , was measured with a parallel plate rheometer.

	Hydrogel polymer density (% w/v)			
	5	10	15	20
<b>Swelling ratio</b>	64.1 ± 0.4	33.9 ± 0.3	28.0 ± 1.1	26.7 ± 0.6
<b>Mesh size (nm)</b>	20.7 ± 0.4	16.1 ± 0.1	14.8 ± 0.3	14.5 ± 0.1
<b>Shear modulus (kPa)</b>	0.6 ± 0.1	1.5 ± 0.0	3.1 ± 0.4	4.5 ± 0.2